JOURNAL OF Materials CHEMISTRY

Coating a bola-amphiphile on amorphous iron nanoparticles

G. Kataby, A. Ulman,[b] M. Cojocaru[a] and A. Gedanken*[a]

[a]*Department of Chemistry, Bar-Ilan University, Ramat-Gan 52900, Israel*
[b]*Department of Chemistry, Polytechnic University, Brooklyn, NY 11201. E-mail: gedanken@mail.biu.ac.il*

Received 9th February 1999, Accepted 23rd April 1999

A bola-amphiphile surfactant, containing a carboxylic acid at one end of the molecule and a thiol at the other, was bonded to nanoparticles of amorphous iron. The bonding of both functional groups was verified by FTIR and XPS measurements. TPD measurements exhibited three temperatures at which molecules are removed from the surface of the iron nanoparticles. The highest temperature, *ca.* 360 °C, is assigned as the temperature at which molecules bonded simultaneously at both ends are desorbed from the surface.

Introduction

The coating of surfaces and particles by the self-assembly and Langmuir–Blodgett techniques has been extensively studied.[1–9] Various experimental methods have been used to probe the mode of bonding between the substrate and the surfactant. Innumerable studies were directed towards amphiphiles carrying one chromophoric end-group. However, it is more attractive, while understanding the nature of the bonding between the substrate and different surfactants, to examine the bonding with a bola-amphiphile. Such a coating can provide two different products. The first is due to the anchoring of one functional group to the substrate, leaving the other free. The second is *via* the bonding of both ends to the substrate. In the first case, the free end-group can be useful for further chemical modifications such as formation of a second layer, hydrolysis, esterification and other reactions.

Coating of bola-amphiphiles on various substrates has already been studied. Chidsey and Loiacono[10] have coated a gold surface with a bifunctional decanethiol. The chemical bonding occurred *via* the sulfur attachment, while the second chromophore (OH, COOH and CN) was left at the outer surface. Structural and electrochemical properties were measured for these surfactants. Schiffrin and coworkers[11] have coated derivatives of dithiazone on gold and ITO electrodes and measured their cyclic voltammetric and other spectroscopic properties. They have also deposited dithiols on gold nanoparticles.[11] Similar bifunctional molecules (*e.g.* with $CONH_2$ and CO_2CH_3 end-groups) having 15 methylene groups were coated on gold surfaces by Nuzzo *et al.*,[12] who conducted IR, XPS, ellipsometry and TPD (temperature programmed desorption) measurements on the coated surface. The films, bonded through the sulfur atom, provide a uniform set of material structures, which differ in the nature of the exposed functionality at the ambient surface. A comparison between 16-mercaptohexadecanoic acid[13] and 4-mercaptobenzoic acid on gold surfaces revealed that the presence of the aromatic group inhibits the formation of hydrogen-bonded dimers or aggregates of carboxylic acid groups that always exist in monolayers based on alkanoic acids. Allara *et al.*[14] have coated a dicarboxylic acid containing 30 CH_2 groups, 1,32-dotriacontanedioic acid, on a freshly prepared silver surface. The presence of the 1703 cm^{-1}, C=O stretching mode of the CO_2H moiety, along with the 1400 and the 1514 cm^{-1} carboxylate modes, indicates that there are two kinds of chain ends. The first is anchored through a carboxylate chemically bound to the silver surface whilst the second type are free CO_2H groups. Contact angle measurements indicate a loop structure for the coated molecule. Disubstituted[15] and trisubstituted benzenes have been deposited on Mg oxide and Al oxide and studied by inelastic electron tunneling microscopy (IETS).

In all the above-mentioned investigations, flat surfaces were exposed to α,ω-type surfactants, but the only work in which a bola-amphiphile was bonded to particle surfaces in general, and to nanoparticles, in particular, is that of Liu and Xu.[16] They have deposited 16-mercaptohexadecanoic acid (MHA) on the surface of γ-Fe_2O_3 nanoparticles using the self-assembly technique. The MHA was anchored to the iron oxide surface by chemical bonding between the carboxylate end-group and the iron, leaving the thiol group free as the ambient surface.

When iron pentacarbonyl[17,18] is sonicated under argon or under air, amorphous nanoparticles of Fe and Fe_2O_3 respectively are produced. We have recently shown that the self-assembly[19–23] method can be used to coat these nanoparticles with surfactants such as octadecyltrichlorosilane (OTS), sodium dodecylsulfate (SDS), thiols and alcohols. The importance of the amorphous form in bonding the various functional groups was demonstrated when commercial submicronic iron or even nanocrystalline iron could not be coated by some of the above-mentioned functional groups. We have attributed the reactivity of amorphous iron to coordinatively unsaturated sites.

The nature of the surface of the iron nanoparticles and the extent of its oxidation is discussed in great detail elsewhere.[21] In short, we claim that, although it is partially oxidized, it does not reach the oxidation state of +3. These results are also demonstrated in the TPD spectrum of thiol-coated iron and thiol-coated Fe_2O_3 where different products are desorbed from the surfaces.[22]

In the present work, we have coated a bola-amphiphile, 11-mercaptoundecanoic acid (MUDA), $HS(CH_2)_{10}COOH$, on the surface of amorphous iron nanoparticles. The coated particles were examined by TGA, DSC, TPD, FTIR, XPS and magnetic measurements. A bonding pattern of MUDA to the iron substrate is proposed in light of these results.

Experimental

The preparation of amorphous iron nanoparticles has been described elsewhere.[17b] In brief, a 1 M solution of $Fe(CO)_5$ in decane was sonicated (Sonics and Materials VC-600, Ti horn, 20 kHz, 100 W cm^{-2}) under argon for 3 h at −90 °C. Great care was taken to minimize oxidation of the product in further steps. Coating with MUDA was carried out in an ethanolic solution, with an Fe : MUDA molar ratio of 12 : 1.

The TGA analysis was done using a Mettler TG-50, and DSC measurements were carried out on a Mettler DSC-30. Mass spectrometic measurements were carried out on a Fisons

VG Instrument (AutoSpec E). The MS-spectra were obtained by direct insertion of the solid probe into the CI ion source. The reagent gas used was methane. Room temperature FTIR spectra were recorded on a Nicolet (Impact 410) spectrometer. The measurements were performed using KBr pellets. The magnetization loop measurements were conducted at room temperature using an Oxford Instruments vibrating sample magnetometer (VSM).

X-Ray photoelectron spectroscopy measurements were carried out using a 5600 Multi-technique System (PHI, US). The samples were irradiated with an Al-Kα approximately monochromated source (1486.6 eV), and the outcoming electrons were analyzed by a Spherical Capacitor Analyzer employing a pass energy of 11.75 eV. The samples were analyzed at the surface after a few minutes of sputter cleaning with a 4 kV Ar^+ ion gun. The sputtering rate was 20 Å min^{-1} (on SiO_2). All the samples were positively charged during measurements. This charging was compensated for by using a charge neutralizer with reference to the C 1s peak of hydrocarbons (*ca.* 284.8 eV).

Results and discussion

The investigations into the nature of the chemical bonding of the bola-amphiphile will be discussed first.

FTIR results

The FTIR spectrum of MUDA bonded to the iron nanoparticles and the unbonded MUDA spectrum are presented in Fig. 1, in the 1000–1800 cm^{-1} range. A large shift from 1700 to 1540 and 1400 cm^{-1} is observed for the carbonyl group upon bonding of MUDA to the iron particle. This indicates the formation of the carboxylate anion, with both oxygens bonded to the iron on the surface. It is worth pointing out that almost the same shift was reported[16] for 16-MHA coated on γ-Fe_2O_3, where the carbonyl band at 1703 cm^{-1} was replaced by peaks at 1527 and 1433 cm^{-1}. The bonding of the carboxylic end to the substrate is therefore demonstrated unequivocally. Fig. 2 presents the FTIR spectrum of the bare MUDA molecule and that of MUDA-coated iron, in the wavenumber region 2450–3000 cm^{-1}. The peak centered at 2558 cm^{-1} in the unbonded MUDA spectrum is assigned to the S–H stretching vibration. This peak is absent from the MUDA-coated iron spectrum, attesting to the formation of a thiolate ion bonded to the iron surface. Thus, the FTIR analysis presents evidence for the formation of chemical bonds to the surface through both ends of the surfactant.

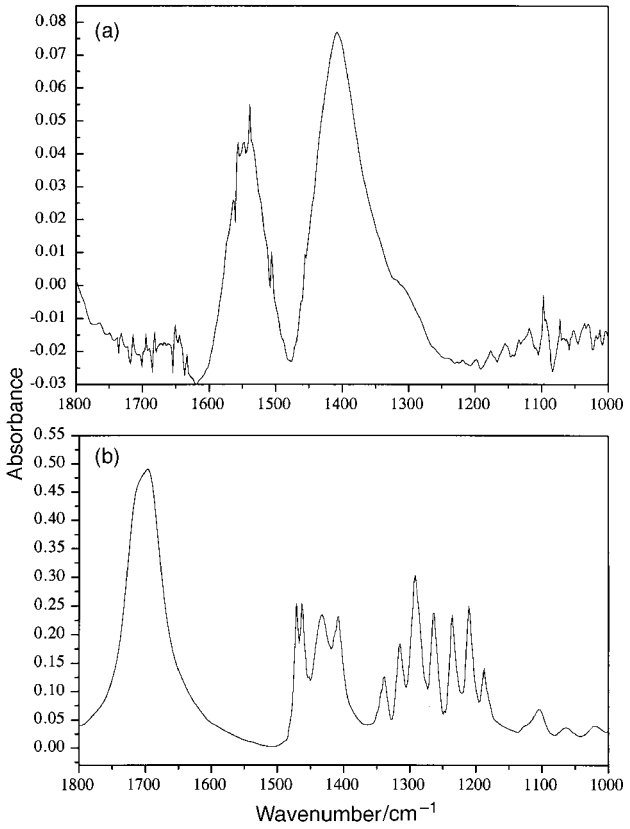

Fig. 1 FTIR spectra of (a) MUDA-coated iron and (b) MUDA in the 1000–1800 cm^{-1} region.

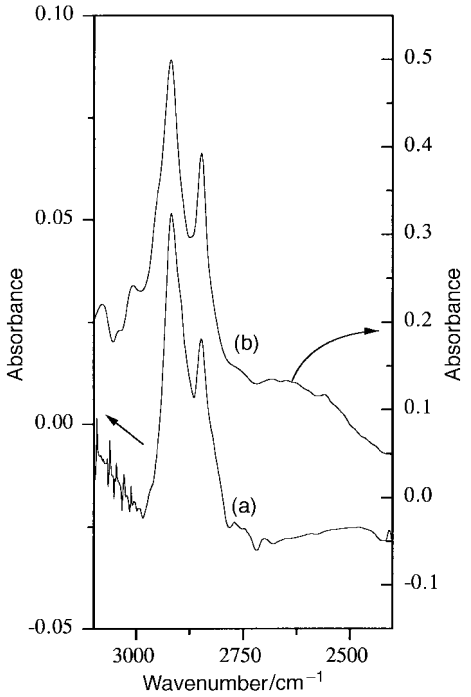

Fig. 2 FTIR spectra of (a) MUDA-coated iron and (b) MUDA in the 2450–3000 cm^{-1} region.

XPS results

The XPS spectra of MUDA and the MUDA-coated iron particles were measured in the Fe 2p, O 1s and S 2p energy regions. Liu and Xu,[16] who also used XPS measurements for establishing the bonding between 16-MHA and Fe_2O_3, did not observe binding of the S–H group to the iron atom. They did, however, observe the XPS peak due to S 2p at 163.7 eV, *i.e.* the free S–H group. In Fig. 3 we present the S 2p XPS spectrum of the MUDA-coated iron particles. The spectrum

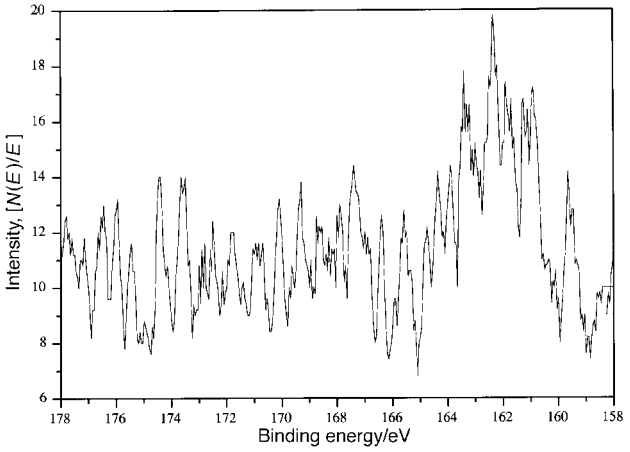

Fig. 3 S 2p XPS spectrum of MUDA-coated iron.

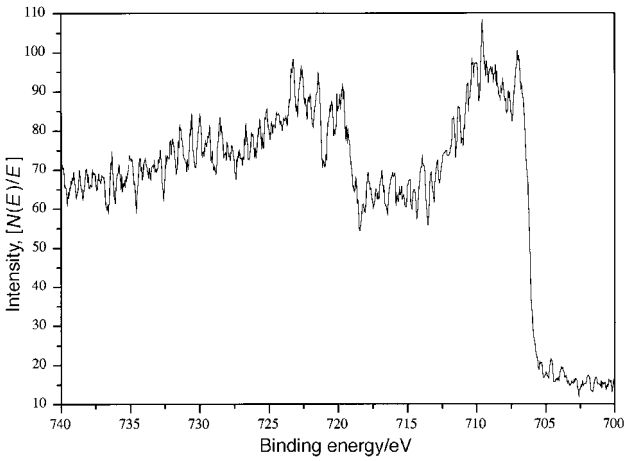

Fig. 4 Fe 2p XPS spectrum of MUDA-coated iron.

was recorded after 3 min of sputtering the surface of the particles with argon ions. The peak obtained for S 2p was detected at 161.6 eV. This energy is close to that reported[16,24] for an Fe–S moiety and is far from that of free S–H. The Fe 2p spectrum is presented in Fig. 4. It was also measured after 3 min of sputtering. Two distinct bands are observed for the $2p_{3/2}$ transition. The first, at 707 eV, is characteristic of the zero-valent iron core. The second peak appears at 710.3 eV and indicates bonding of the surface iron atoms to the surfactant. The 710.3 eV band points to an oxidized iron surface. However, the position of this peak does not give any information about the nature of the bonded groups or for the fact that, in our case, two functional groups are indeed bonded to the iron.

When the spectrum of the untreated particles was compared with the XPS spectrum of the as prepared MUDA-coated iron, we did not observe the 707 eV peak. This indicates that the iron on the surface is oxidized, as also observed in ref. 21.

TPD measurements

In Fig. 5, we present the dependence of the total ion current of the desorbed molecules on temperature. The trace reveals four desorption peaks that were further mass analyzed. The peaks were detected at around 150, 200, 270 and 360 °C. The lowest temperature peak was interpreted as being related to desorption of the solvent from the iron surface. The second desorption peak was attributed to the rupture of the S–Fe bonds. This interpretation is based on previous TPD and TGA results,[19,20] in which the inflection point in the weight-loss curve for thiol-coated iron particles was detected at 200 °C.

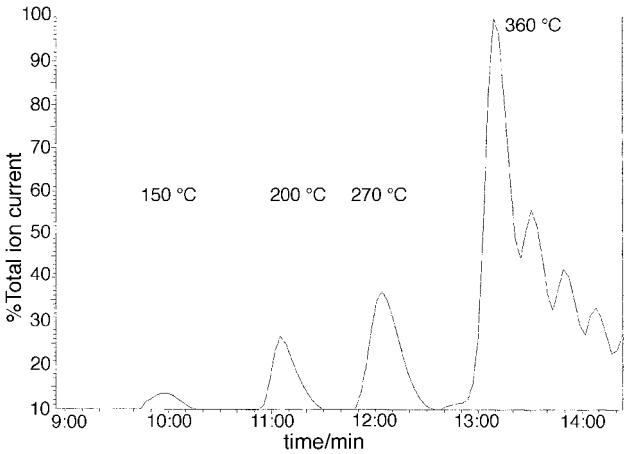

Fig. 5 Total ion current of MUDA-coated iron as a function of temperature.

The third peak, at 270 °C, is associated with breaking of the Fe–O–CO bond. This is in agreement with the corresponding TGA data from carboxylic acids coated on iron,[23b] where the inflection point in the weight-loss spectrum for heptanoic acid-coated iron particles was detected at 280 °C. The reason that carboxylic acids form stronger bonds with the amorphous iron than do thiols is perhaps due to the chelating nature of the carboxylate ion, which involves the two oxygen atoms in bonding to the iron. This is also in agreement with previous studies,[16] where only the carboxylic functionality was found to bond to γ-Fe_2O_3.

The 200 and 270 °C desorption bands are related to molecules bonded to iron through only one functional group. Indeed, the mass analyzed spectra (Fig. 6) of these two peaks show the same mass, 217 u, corresponding to the $(M-1)^+$ parent molecule. The intensities of the 217 u peaks measured at the two temperatures are different and will be discussed below. The desorption peak at 200 °C is therefore assigned to the MUDA molecule anchored to the iron through a S–Fe bond leaving a free COOH group at the outer surface. This assignment raises the question of the disappearance of the 1700 cm^{-1} peak in the IR spectrum of MUDA-coated iron. The absence of the 1700 cm^{-1} peak for molecules that are bonded to the iron only through the thiol chromophore (leaving a free carboxylic acid in the outer space) is mirrored by the small desorption peak at 200 °C. When the area under the peak is evaluated, it is estimated that only 8% of the molecules are bonded in this way. Such a weak peak is not likely to be detected in the IR spectrum.

The strongest TPD band at 360 °C can be interpreted as associated with molecules bonded to the iron particles *via* both ends. This higher temperature is required since simultaneous rupture of two bonds from the iron nanoparticle must occur. The bonding of MUDA at both ends to iron atoms can be envisioned as interparticle or intraparticle bonding. In the interparticle bonding model, the MUDA molecule is stretched and bonded to two iron particles, which will then be separated by eleven carbon atoms. In the intraparticle bonding model, both ends are connected to the same particle, imposing a bend in the alkyl chain. The mass-analyzed spectrum (Fig. 7) reveals a molecular peak at 341 u. This mass fits well (error of 0.5 ppm) with the empirical formula, $C_{21}H_{41}SO$. The two possible structures corresponding to this mass are presented in Scheme 1.

The scheme shows fragmentation ions which are observed at $m/z = 307$ and 309 and correspond to structures **a** and **b**, respectively. The presence of the peak at $m/z = 309$ in the B/E constant-linked scanning measurement is supportive of structure **b**.

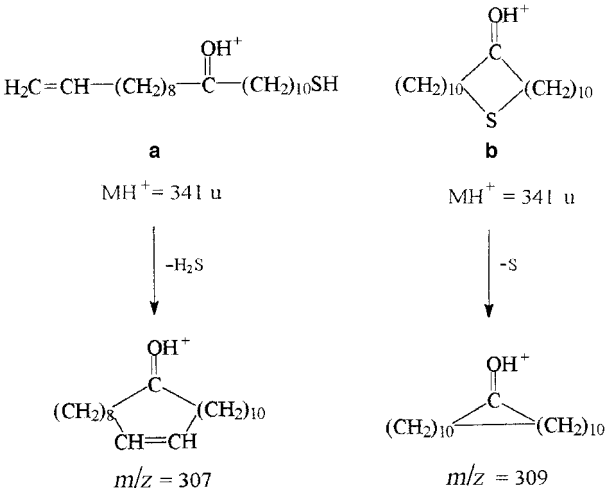

Scheme 1

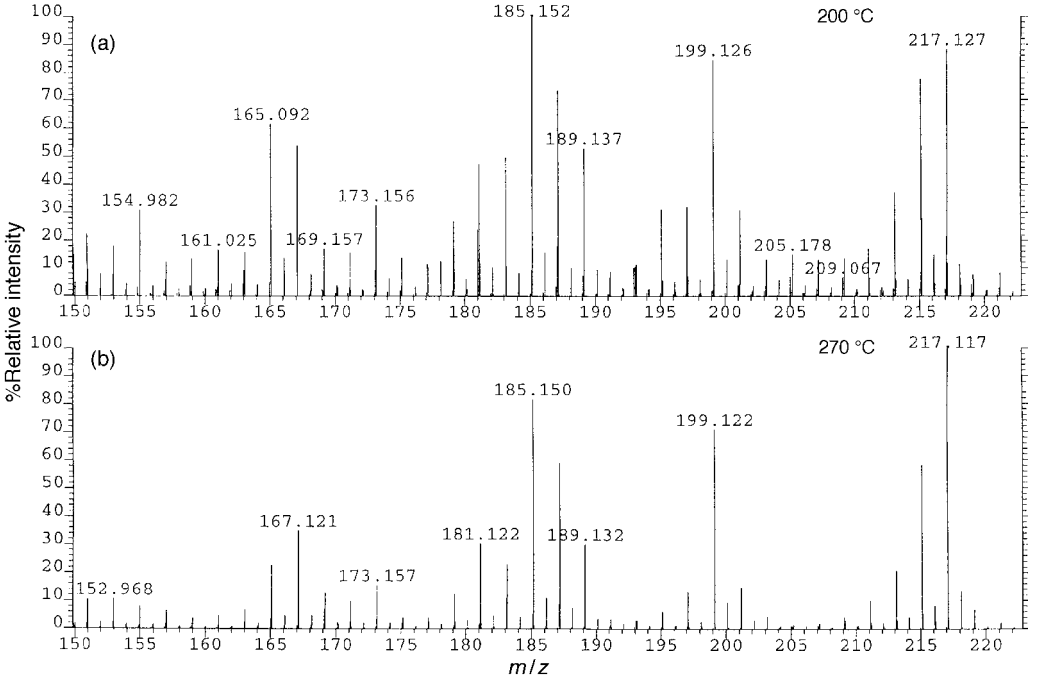

Fig. 6 CI/CH_4 mass spectra of MUDA-coated iron at (a) 200 °C and (b) 270 °C.

The formation of a 'dimeric' species also favors the intraparticle binding option of MUDA to the iron particle. To eliminate the possibility that the desorbed entity is a result of dimerization of the parent molecule under MS conditions, we have also examined the mass spectrum of the parent molecule. The only peaks due to dimeric moieties that were observed were at $m/z=419$ and 401, corresponding to the loss of one or two water molecules from the $(M_2H)^+$ ion, respectively (a common ion molecule reaction occurring under MS conditions). So, the peak at $m/z=341$ (Fig. 8) arises only from MUDA-coated iron.

This further substantiates our claim for a desorption process involving both end-groups of MUDA. Whether the 22 membered ring has already been formed on the iron surface or occurs during the desorption process is still under investigation.

The complex structure of the TPD spectrum and the evidence provided for the bonding of the bola-amphiphile at both ends again raises the issue of the comparison between the bonding capabilities of the crystalline and amorphous nanoparticles. The reactivity of the amorphous iron particles is demonstrated in the bonding of the two ends of the molecule to the substrate, whereas crystalline γ-Fe_2O_3 bonded with MHA through only the carboxylate group, leaving the thiol unbonded. We have attributed this high reactivity of the amorphous material to coordinatively unsaturated surface sites existing in the amorphous nanoparticles.

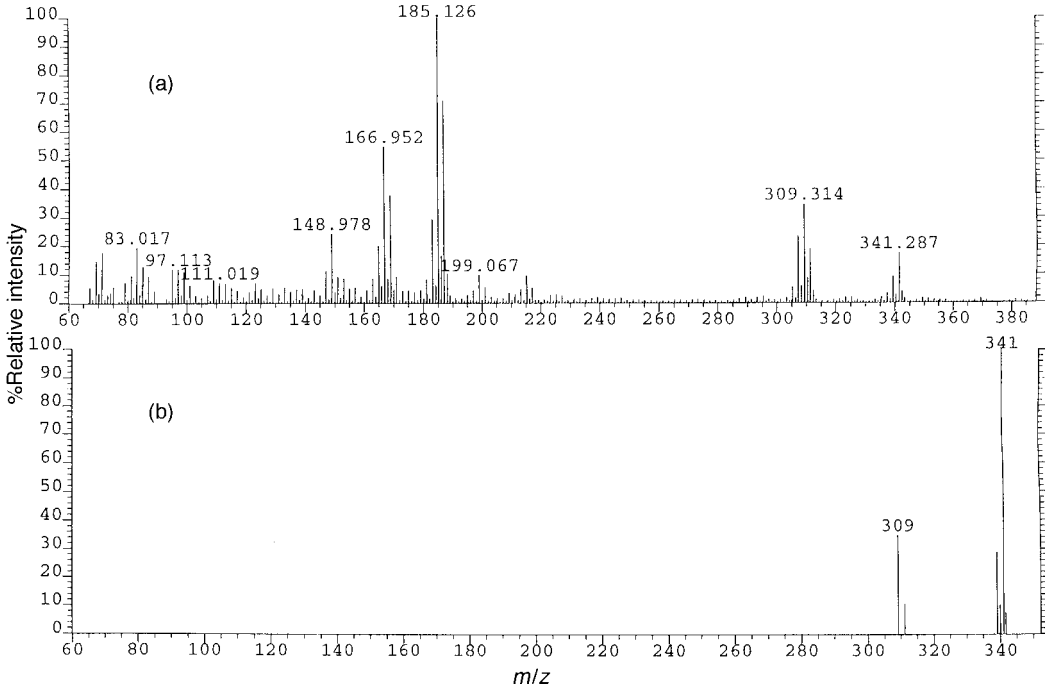

Fig. 7 (a) CI/CH_4 mass spectrum of MUDA-coated iron at 370 °C. (b) B/E constant linked scanning from $m/z=341$ under the same ionization conditions.

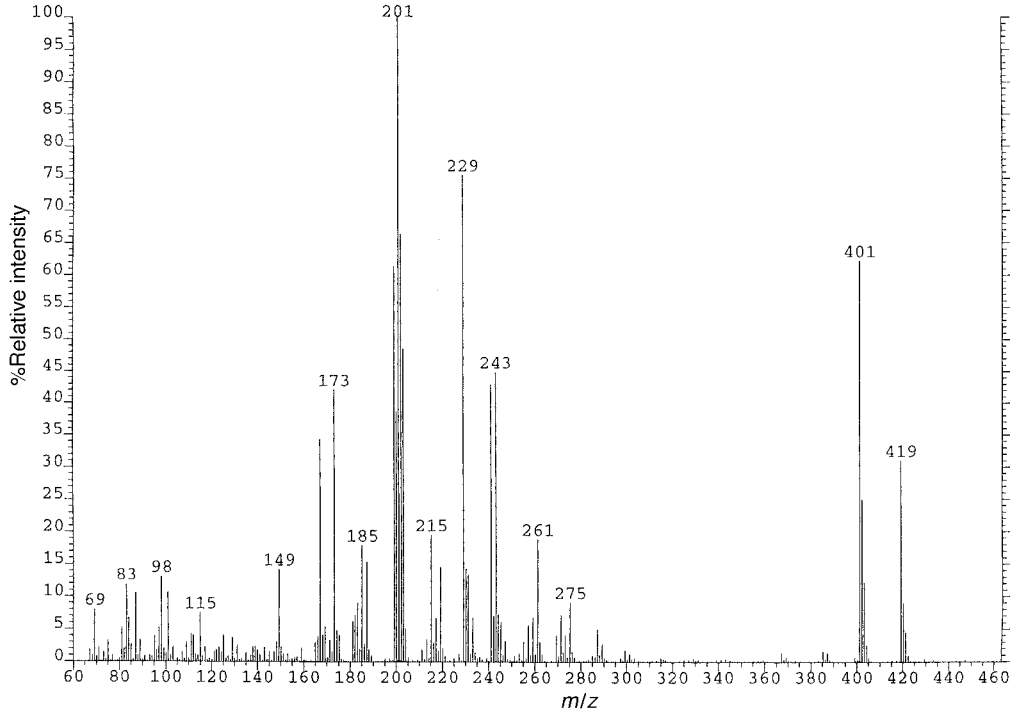

Fig. 8 CI/CH_4 mass spectrum of MUDA.

TGA and DSC measurements

The TGA spectrum of MUDA-coated iron particles is presented in Fig. 9. The spectrum shows an unstructured weight loss of 16% over the 200–450 °C temperature range. However, when the derivative of the TGA curve is calculated, two peaks at 282 and 363 °C are detected which correspond very well with the TPD peaks at 270 and 360 °C. The DSC spectrum of MUDA-coated iron is depicted in Fig. 10. The strongest feature in the spectrum is the exothermic peak at 290 °C. This is attributed to the transition of the amorphous iron nanoparticles to the crystalline phase. This peak is detected in the spectrum of octadecanethiol-coated iron particles at 313 °C. For bare iron particles the exothermic peak is observed at 308 °C.[17] The temperature shift results from the broad endothermic peak overlapping the exothermic band, preventing the location of the true position of the exothermic peak. The first endothermic peak, which is observed at 100 °C, is related to the desorption of the various solvents used in the coating and washing processes. Endothermic shoulders are seen at 210 and 260 °C. They correspond well to the above-mentioned TPD peaks related to the rupture of the single S–Fe and carboxylate–Fe bonds, respectively. The deep endothermic peak centered at 350 °C is related to the TPD peak at 360 °C, corresponding to the desorption of the dimeric species. This endothermic peak is responsible for the shift to lower temperatures of the crystallization temperature.

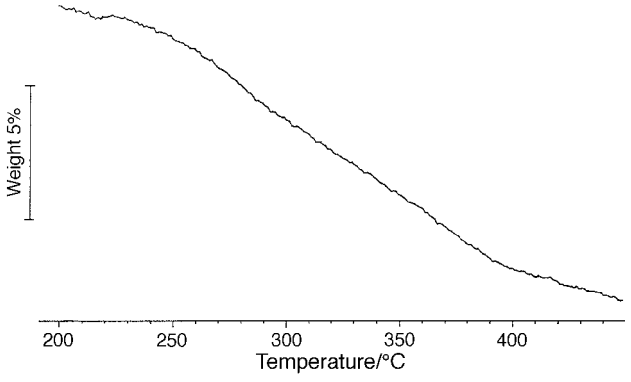

Fig. 9 TGA spectrum of MUDA-coated amorphous iron nanoparticles in the range 200–450 °C. The heating rate is 2 °C min^{-1}. The carrier gas is 99.999% N_2.

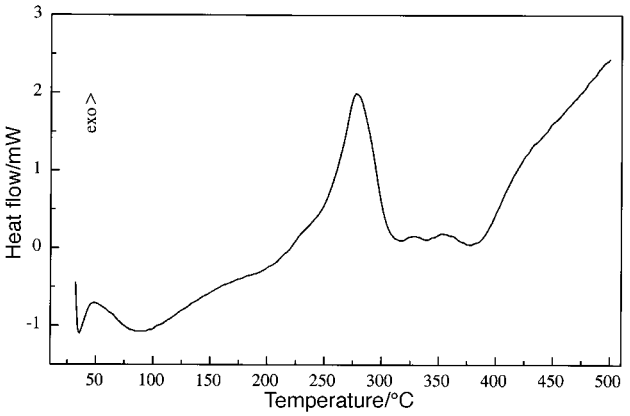

Fig. 10 DSC spectrum of MUDA-coated amorphous iron nanoparticles. The heating rate is 10 °C min^{-1}. The carrier gas is 99.999% N_2.

Magnetic measurements

The hysteresis loop of MUDA-coated iron particles appears almost identical to the corresponding magnetization loops of thiol-coated iron particles and alcohol-coated iron particles.[23a] This typical behavior,[25] which has been observed previously and is characterized by the lack of hysteresis and the absence of saturation of the magnetization, is also observed in Fig. 11. This behavior is due to the superparamagnetic nature[26–29] of the particles, which has been discussed previously.[23] The magnitude of the magnetization (at 15 kG) is the same as those observed for other thiol-coated iron particles.

Conclusions

The current work has investigated the bonding of a bola-amphiphile to nanophase amorphous iron particles. The

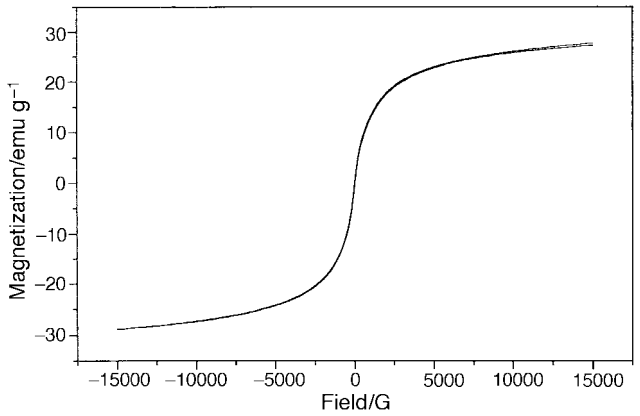

Fig. 11 Magnetization loop of MUDA-coated amorphous iron particles.

existence of chemical bonds between iron and the S–H and carboxylic end-groups has been demonstrated qualitatively through the IR and XPS spectra. The quantitative picture is revealed *via* the TPD spectrum, which depicts three major peaks, leading to three different products. The first peak, which shows a desorption of molecules at 200 °C, is associated with molecules bonded through the S–H chromophore, leaving an outer free carboxylic group. The number of molecules bonded this way amounts to 8%, as obtained from the peak area. The molecules bonded through the carboxylic moiety amount to 12% and are desorbed at 280 °C. This is in agreement with Xu and Liu, who also reported the formation of stronger bonds between the carboxylate and Fe_2O_3.[16] Finally, 80% of the molecules, which are desorbed at 360 °C are bonded at the two ends simultaneously.

We can foresee two geometrical possibilities for the structure of this species. The first is a stretched MUDA bonded to different iron nanoparticles at either end. The second is a bent molecule with both ends bonded to one iron nanoparticle. We should mention that the detection of 'dimeric' desorbed species is an indication in favor of a bent molecule adsorbed onto a single iron nanoparticle. However, this question is still under investigation.

Acknowledgments

This research was partially supported by Grant No. 94–00230 from the U.S.–Israel Binational Science Foundation (BSF), Jerusalem, Israel. We thank Dr. L. Burstein for XPS measurements in the Wolfson Applied Materials Research Center, Tel-Aviv University. We also thank Dr. S. Hochberg for her editorial assistance.

References

1 C. D. Bain and G. M. Whitesides, *J. Am. Chem. Soc.*, 1989, **111**, 7164.
2 E. Delmarche, B. Michel, H. Kang and C. Gerber, *Langmuir*, 1994, **10**, 4103.
3 M. J. Hostetler, J. J. Stokes and R. W. Murray, *Langmuir*, 1996, **12**, 3604.
4 P. E. Laibinis, M. A. Fox, J. P. Folkers and G. M. Whitesides, *Langmuir*, 1991, **7**, 3167.
5 A. Ulman, S. D. Evans, Y. Shnidman, R. Sharma, J. E. Eilers and J. C. Chang, *J. Am. Chem. Soc.*, 1991, **113**, 1499.
6 C. S. Weisbecker, M. V. Merrit and G. M. Whitesides, *Langmuir*, 1996, **12**, 3763.
7 R. G. Nuzzo, B. R. Zegarski and L. H. Dubois, *J. Am. Chem. Soc.*, 1987, **109**, 733.
8 C. J. Sandorff, S. Garoff and K. P. Leung, *Chem. Phys. Lett.*, 1983, **96**, 547.
9 G. E. Poirier and E. D. Pylant, *Science*, 1996, **272**, 1145.
10 C. E. D. Chidsey and D. Loiacono, *Langmuir*, 1990, **6**, 682.
11 (*a*) F. Mirkhalaf, D. Whittaker and D. J. Schiffrin, *J. Electroanal. Chem.*, 1998, **452**, 203; (*b*) M. Brust, D. Bethell, C. J. Kiely and D. J. Schiffrin, *Langmuir*, 1998, **14**, 5425.
12 R. G. Nuzzo, L. H. Dubois and D. L. Allara, *J. Am. Chem. Soc.*, 1990, **112**, 558.
13 S. E. Creager and C. M. Steiger, *Langmuir*, 1995, **11**, 1852.
14 D. L. Allara, S. V. Atre, C. A. Elliger and R. G. Snyder, *J. Am. Chem. Soc.*, 1991, **113**, 1852.
15 (*a*) N. M. D. Brown, B. J. Meenan and G. M. Taggart, *Spectrochim. Acta*, *Part A*, 1991, **47**, 219; (*b*) N. M. D. Brown, B. J. Meenan and G. M. Taggart, *Spectrochim. Acta*, *Part A*, 1991, **47**, 387.
16 Q. Liu and Z. Xu, *Langmuir*, 1995, **11**, 4617.
17 (*a*) K. S. Suslick, P. F. Schubert and J. W. Goodale, *J. Am. Chem. Soc.*, 1981, **103**, 7342; (*b*) K. S. Suslick, S.-B. Choe, A. A. Cichowlas and M. W. Grinstaff, *Nature*, 1991, **353**, 414.
18 M. W. Grinstaff, A. A. Cichowlas, S.-B. Choe and K. S. Suslick, *Ultrasonics*, 1992, **30**, 168.
19 O. Rozenfeld, Yu. Koltypin, H. Bamnolker, S. Margel and A. Gedanken, *Langmuir*, 1994, **10**, 627.
20 G. Kataby, Yu. Koltypin, X. Cao and A. Gedanken, *J. Cryst. Growth*, 1996, **166**, 760.
21 G. Kataby, Yu. Koltypin, Y. Rothe, J. Hormes, I. Felner, X. Cao and A. Gedanken, *Thin Solid Films*, 1998, **333**, 41.
22 G. Kataby, T. Prozorov, Yu. Koltypin, C. N. Sucenik, A. Ulman and A. Gedanken, *Langmuir*, 1997, **13**, 6151.
23 (*a*) G. Kataby, A. Ulman, R. Prozorov and A. Gedanken, *Langmuir*, 1998, **14**, 1512; (*b*) G. Kataby, M. Cojocaru, R. Prozorov and A. Gedenken, *Langmuir*, 1999, **15**, 1703.
24 J. F. Moulder, W. F. Stickle, P. E. Sobol and K. D. Bomben, *Handbook of X-Ray Photoelectron Spectroscopy*, Perkin-Elmer Corporation, MN.
25 X. Cao, Yu. Koltypin, G. Kataby, R. Prozorov and A. Gedanken, *J. Mater. Res.*, 1995, **10**, 2952.
26 A. Marmur, W. Chen and G. Zografi, *J. Colloid Interface Sci.*, 1985, **113**, 114.
27 B. L. Maschhof and N. R. Armstrong, *Langmuir*, 1991, **7**, 693.
28 S. Morup, *Europhys. Lett.*, 1994, **28**, 671.
29 T. Ishikawa, W. Y. Cai and K. Kandor, *J. Chem. Soc.*, *Faraday Trans.*, 1992, **88**, 1173.

Paper 9/01113G